# A Relaxed Direct-insertion Downscaling Method For Discrete-in-time Data Assimilation

Emine Celik[1] and Eric Olson[2]

August 11, 2026

[1]*Department of Mathematics, Sakarya University*
*54050 Sakarya, Türkiye*
[2]*Department of Mathematics and Statistics, University of Nevada, Reno*
*Reno, NV 89557, USA*

Email addresses: `eminecelik@sakarya.edu.tr, ejolson@unr.edu`

**Abstract**

This paper introduces a relaxed direct-insertion method for discrete-in-time data assimilation that overcomes the constraint on observation frequency in the spectrally-filtered direct-insertion downscaling method. Numerical simulations demonstrate that taking the relaxation parameter proportional to the time between observations allows one to vary the observation frequency over a wide range while maintaining convergence of the approximating solution to the reference solution. Under the same assumptions we obtain a new connection between discrete-in-time direct-insertion methods for data assimilation and continuous-in-time nudging. Namely, we analytically prove that taking the observation frequency to infinity results in continuous-in-time nudging.

# 1 Introduction

Our focus is that of a well-posed dissipative dynamical system

$$\frac{dU}{dt} = \mathcal{F}(U) \qquad \text{with} \qquad U(t_0) = U_0 \tag{1.1}$$

where the initial condition $U_0$ is unknown but for which a time sequence of partial observations of $U(t)$ are available at times $t = t_n$.

Following [2], [27], related research, the references therein and in particular [6], we consider the concrete setting of the incompressible two-dimensional Navier–Stokes equations. These equations provide an example of a dynamical system of the form (1.1) that is simpler than atmospheric or ocean models but with similar nonlinear dynamics. Other systems for which a growing body of analytic and numerical results are available include Rayleigh–Bénard convection studied by Farhat, Lunasin and Titi in [11] (see also Farhat, Glatt-Holtz, Martinez, McQuarrie and Whitehead [12] and Hammoud, Le Maître, Titi, Hoteit and Knio [18]) and also the surface quasi-geostrophic equations studied by Jolly, Martinez and Titi in [22] (see also [23]) among others. Although our study focuses on the two-dimensional Navier–Stokes equations, we hope the resulting intuition and conclusions will apply to these other systems as well as the operational models used in practical applications.

We begin with the spectrally-filtered discrete-in-time downscaling data assimilation algorithm introduced in [6] in the context of the incompressible two-dimensional Navier–Stokes equations. We state this algorithm here as

**Definition 1.1.** Given an increasing sequence $t_n$ of observation times, the approximating solution $u(t)$ obtained by *spectrally-filtered discrete-in-time data assimilation* is

$$u(t) = S(t - t_n)u_n \qquad \text{for} \qquad t \in [t_n, t_{n+1}),$$

where $u_0 = JU(t_0)$ and

$$u_{n+1} = (I - J)S(t_{n+1} - t_n)u_n + JU(t_{n+1}).$$

Here $S$ is the solution operator for (1.1) and $JU$ represents the spectrally-filtered observations of the reference solution.

The exact form of $J$ is described in (2.7), (2.10) and (2.11) below and formed by projecting and smoothing a simpler interpolant $I_h$ of the observations. Although $J$ is linear, it is not a projection. We consider this an important aspect of $J$ that reflects how signal processing might affect observations in realistic applications.

This is a direct-insertion method that recovers unobserved lengthscales by inserting new observational measurements as they are available into the current estimate of the state. The spectral filter helps ensure no high-resolution artifacts are present in the interpolated observational data that might damage the approximation obtained by the numerical model as it is integrated forward in time. From a theoretical point of view, the filtering is needed to obtain suitable estimates in the higher Sobolev norms used to show convergence of the approximating solution to the reference solution over time.

Intuitively more frequent observations should make the predicted state obtained from data assimilation more accurate. For example, measuring the state of the atmosphere more frequently in weather forecasting should—provided a reasonable algorithm is used—allow an approximating solution to track the reference solution more accurately. However, although more frequent observations represent greater knowledge about the reference solution, preliminary calculations presented in Figure 1 of Section 2 show the data assimilation algorithm given by Definition 1.1 performs worse when the data is inserted more frequently.

In this paper we address the difficulty of how to assimilate more frequent observations by introducing a relaxation parameter into Definition 1.1. Intuitively, when there are more observations available it makes sense to assign a lesser weight to each. We therefore modify the discrete-in-time data assimilation algorithm studied in [6] by introducing a parameter which will depend on the time between successive observations. In details suppose the observations occur at an increasing sequence $t_n$ of times. Choose $\kappa_n \in [0, 1]$ and modify the recurrence defining $u_{n+1}$ in Definition 1.1 to obtain

**Definition 1.2.** Given an increasing sequence $t_n$ of observation times, the approximating solution $\tilde{u}(t)$ obtained by *$\kappa$-relaxed spectrally-filtered discrete-in-time data assimilation* is

$$\tilde{u}(t) = S(t - t_n)\tilde{u}_n \qquad \text{for} \qquad t \in [t_n, t_{n+1}),$$

where $\tilde{u}_0 = JU(t_0)$ and

$$\tilde{u}_{n+1} = (I - \kappa_n J)S(t_{n+1} - t_n)\tilde{u}_n + \kappa_n JU(t_{n+1}). \tag{1.2}$$

Note that taking $\kappa_n = 1$ independent of $n$ in Definition 1.2 recovers Definition 1.1. We remark that $\kappa_n$ plays a role similar to the term used by the Bayesian update for the ensemble Kalman filter which balances the tradeoff between the accuracy of the predicted state and the quality of the observations (see, for example, Evensen [10] or Grudzien and Bocquet [17]). The context considered here, however, is that of noise-free observations with exactly known dynamics. Thus, it is not noise and model error which lead us to introduce $\kappa_n$ but the balance between lack of orthogonality in a rough interpolant and smoothing by the dynamics. Although noise and model error are important for applications, the present research studies only the noise-free case.

To discern how $\kappa_n$ should depend on $n$ compare the data-assimilation method given in Definition 1.2 to the continuous nudging method of [2] given by

$$\frac{dv}{dt} = \mathcal{F}(v) + \mu J(U - v), \quad \text{where} \quad v(t_0) = \tilde{u}_0. \tag{1.3}$$

Note the effect of the nudging in (1.3) over the interval $[t_n, t_{n+1}]$ is approximately

$$\int_{t_n}^{t_{n+1}} \mu J(U - v)dt \approx (t_{n+1} - t_n)\mu J\big(U(t_n) - v(t_n)\big). \tag{1.4}$$

Since at the beginning of the same interval (1.2) kicks the approximation by

$$-\kappa_n JS(t_n - t_{n-1})\tilde{u}_{n-1} + \kappa_n JU(t_n) = \kappa_n J\big(U(t_n) - \tilde{u}(t_n^-)\big),$$

it is natural to take $\kappa_n = (t_{n+1} - t_n)\mu$. The numerical and theoretical analysis of Definition 1.2 under this identification is the main focus of the present research.

We remark for the continuous nudging method (1.3) to asymptotically recover $U$ it is necessary for $\mu$ to be sufficiently large and the resolution $h$ of the observations sufficiently fine. Our goal is for $k_n$ to under-relax the assimilation step given by (1.2) to handle the case of more frequent discrete-in-time observations. After fixing $\mu$ the requirement that $k_n \le 1$ can then be viewed as a further bound on the time between observations.

For simplicity suppose the time between observations is fixed to be $\delta$ for some $\delta > 0$. Thus, $t_n = t_0 + \delta n$ and $\kappa_n$ is independent of $n$. This will be our working assumption in all that follows. Dropping subscripts we take $\kappa_n = \kappa$ where $\kappa = \mu\delta$. Since $\kappa \to 0$ as $\delta \to 0$, the more frequent the observations the smaller the update based on them. Our main theoretical result, stated as Theorem 1.5 below, proves the $\kappa$-relaxed discrete-in-time data assimilation algorithm given by Definition 1.2 converges to continuous nudging (1.3) as $\delta \to 0$.

The limit studied in the present paper takes $\delta \to 0$ while holding $\mu$ fixed. This can be contrasted to holding $\kappa$ fixed which then implies $\mu \to \infty$ as $\delta \to 0$ and intuitively leads to the continuous direct replacement method

$$\frac{d\tilde{v}}{dt} = \mathcal{F}\big((I - \kappa J)\tilde{v} + \kappa JU\big) \quad \text{where} \quad \tilde{v}(t_0) = \tilde{u}_0. \tag{1.5}$$

Along these lines Carlson, Farhat, Martinez and Victor [4] see also Diegel, Li and Rebholz [9] show in the limit $\mu \to \infty$ when $J$ is given by an orthogonal projection that continuous nudging (1.3) converges to (1.5) with $\kappa = 1$.

Larios, Pei and Victor [26] consider time-delayed continuous nudging, hold $\delta$ fixed and then obtain a data assimilation method similar to Definition 1.2 by reducing to zero the length of the time window over which past observations steer the approximation. This provides a different justification for the relaxation parameter $\kappa$ in Definition 1.2 and further motivates the data-assimilation framework that is our focus.

We now describe main theorem proved in [6] for the spectrally-filtered discrete-in-time data assimilation algorithm given by Definition 1.1 whose improvement is the purpose of the present paper. Note that taking $J = P_\lambda$ leads to the discrete-in-time data-assimilation method studied in [20] based on observation of the Fourier modes. In this case the quality of the approximation $u(t)$ does not worsen when measurements are inserted more frequently in time. Thus, lack of orthogonality and smoothness in $J$ appear to be important considerations.

The main result from [6] may be stated as

**Theorem 1.3.** *Let $U$ be a solution to the incompressible two-dimensional Navier–Stokes equations and $u(t)$ be the process given by Definition 1.1. Then, for every $\delta > 0$ there exists $h > 0$ and $\lambda > 0$ depending only on $c_1$, $f$ and $\nu$ such that*

$$|u(t) - U(t)| \to 0 \quad \textit{exponentially in time as} \quad t \to \infty.$$

*Here $c_1$ is the constant appearing in* (2.10).

In the presence of model error and noise the synchronization given by Theorem 1.3 as $t \to \infty$ would be only approximate. While it seems reasonable that observing the reference solution less frequently in time with larger $\delta$ can be compensated for by requiring higher resolution observations with smaller $h$, the difficulty we address with Definition 1.2 is that once the observation period $\delta$ is chosen, the theory does not allow more frequent observations without again adjusting the resolution $h$ and filter parameter $\lambda$.

Ideally, we would like a result for $\tilde{u}$ similar to Theorem 1.3 that relaxes the lower bound on the size of $\delta$. This we state as

**Conjecture 1.4.** *Let $U$ be a solution to the incompressible two-dimensional Navier–Stokes equations and $\tilde{u}(t)$ be the process given by Definition 1.2. Then, for every $\delta_0 > 0$ there exists $h > 0$, $\lambda > 0$ and $\mu > 0$ depending only on $c_1$, $f$ and $\nu$ such that $0 < \delta < \delta_0$ implies*

$$|\tilde{u}(t) - U(t)| \to 0 \quad \textit{exponentially in time as} \quad t \to \infty.$$

*Here $c_1$ is the constant appearing in* (2.10).

As indicated by the numerics in Section 3 such a conjecture indeed seems plausible. Our present theory falls short; however, we are able to prove that $\tilde{u}$ converges to the approximation $v$ given by continuous nudging in the limit that $\delta$ vanishes. Namely, we obtain

**Theorem 1.5.** *Given a reference solution $U$ lying on the global attractor of the incompressible two-dimensional Navier–Stokes equations, let $\tilde{u}$ be the approximating solution obtained by* (1.2) *with $\kappa = \mu\delta$ and let $v$ be obtained by* (1.3). *Then, for every $T > t_0$ it follows that*

$$\sup\big\{\|\tilde{u}(t) - v(t)\| : t \in [t_0, T]\big\} \to 0 \qquad \textit{as} \qquad \delta \to 0.$$

*Moreover, the above result holds for every $J = P_\lambda P_H I_h$ independently of whether $h$, $\lambda$ and $\mu$ have been chosen so $\|v(t) - U(t)\| \to 0$ as $t \to \infty$.*

The above result allows us to take $\delta$ arbitrarily small; however, it does not allow us to show that $|\tilde{u}(t) - U(t)| \to 0$ as $t \to \infty$. Instead we have

**Theorem 1.6.** *There exists $h$, $\lambda$ and $\mu$ such that for every $\varepsilon > 0$ there corresponds $T$ large enough and $\delta_0 > 0$ such that*

$$\|\tilde{u}(T) - U(T)\| < \varepsilon \qquad \textit{for all} \qquad 0 < \delta < \delta_0$$

*and every reference solution $U$ lying on the global attractor.*

The above result is a consequence of Theorem 1.5 combined with Theorem 2 in [2]. We state the proof here to illustrate the application of our present theory.

*Proof of Theorem 1.6.* From Theorem 2 in [2] there exists $h$, $\lambda$ and $\mu$ such that

$$\|v(t) - U(t)\| \to 0 \qquad \text{as} \qquad t \to \infty.$$

Let $\varepsilon > 0$. Therefore, there exists $T$ large enough such that

$$\|v(t) - U(t)\| < \varepsilon/2 \qquad \text{for all} \qquad t \geq T.$$

Now choose $\delta_0 > 0$ in Theorem 1.5 such that

$$\sup\big\{\|\tilde{u}(t) - v(t)\| : t \in [t_0, T]\big\} \leq \varepsilon/2 \qquad \text{for all} \qquad 0 < \delta < \delta_0.$$

It follows that

$$\|\tilde{u}(T) - U(T)\| \leq |\tilde{u}(T) - v(T)| + |v(T) - U(T)| < \varepsilon.$$

This finishes the proof. □

This paper is organized as follows. Section 2 recalls the two-dimensional incompressible Navier–Stokes equations, introduces the functional setting which will be used throughout, the exact form of the interpolant observable $J$ and states some well-known bounds on the reference solution $U$. In Section 3 we study how the optimal value of $\kappa$ depends on $\delta$ numerically and provide evidence for Conjecture 1.4. Section 4 begins with some theoretical preliminaries and ends with the proof of Theorem 1.5. Concluding remarks and directions for future work appear in Section 5.

## 2 Preliminaries

The possibility that inserting observations more frequently in time using Definition 1.1 could lead to lack of synchronization between the approximating solution and reference solution was already noticed in the theoretical analysis presented in [6] and commented on as

> *[Our analysis makes] use of a minimum distance between $t_{n+1}$ and $t_n$ as well as the maximum. Measurements need to be inserted frequently enough to overcome the tendency for two nearby solutions to drift apart, while at the same time the possible lack of orthogonality in our general interpolant observables means measurements should not be inserted too frequently.*

We are further motivated by numerical evidence in Section 3 that the above comment concerning the minimum observation frequency is physical and not merely a limitation of our analytic techniques. To overcome this constraint we introduce the relaxation parameter $\kappa_n$ in Definition 1.2.

The context of the above analysis and present research is the two-dimensional incompressible Navier–Stokes equations with no modeling or observational error. In particular, given the ideal situation of noise-free observations of exact dynamics in which the approximating solution synchronizes with the reference solution over time, our computations show that inserting measurements more frequently can worsen the quality of the approximation to the point where it subsequently fails to synchronize.

Recall the incompressible two-dimensional Navier–Stokes equations given by

$$\frac{\partial U}{\partial t} + (U \cdot \nabla)U - \nu \Delta U + \nabla p = f, \qquad \nabla \cdot U = 0, \tag{2.1}$$

where $U$ is the velocity of the fluid, $\nu$ is the kinematic viscosity, $p$ is the pressure and $f$ is a time-independent body force applied to the fluid. Consider the spatial domain $\Omega$ with $L$-periodic boundary conditions for simplicity.

Recast (2.1) in the functional setting described by Constantin and Foias [7] (see also Robinson [28] or Temam [29]) as follows. Denote by $\mathcal{V}$ the set of all divergence-free $L$-periodic trigonometric polynomials with zero spatial averages. Let $V$ be the closure of $\mathcal{V}$ in $H^1(\Omega, \mathbf{R}^2)$ and $H$ be the closure of $\mathcal{V}$ in $L^2(\Omega, \mathbf{R}^2)$. Denote the dual of $V$ by $V^*$.

Let $A\colon V \to V^*$ and $B\colon V \times V \to V^*$ be continuous extensions of the operators given by $Au = -P_H \Delta u$ and $B(u, v) = P_H(u \cdot \nabla v)$ for $u, v \in \mathcal{V}$ where $P_H$ is the orthogonal projection of $L^2(\Omega)$ onto $H$. Let $\mathcal{D}(A) = \{u \in V : Au \in H\}$ be the domain of $A$ into $H$. Applying $P_H$ to both sides of (2.1) then expresses the Navier–Stokes equations as

$$\frac{dU}{dt} + \nu AU + B(U, U) = f \qquad \text{where} \qquad U(t_0) = U_0 \in V. \tag{2.2}$$

Note in the periodic case $A = -\Delta$ and that we have assumed $P_H f = f$.

The spaces $H$, $V$ and $\mathcal{D}(A)$ can be characterized in terms of Fourier series as $H = V_0$, $V = V_1$ and $\mathcal{D}(A) = V_2$ where

$$V_\alpha = \left\{ \sum_{k \in \mathcal{J}} u_k e^{ik \cdot x} : \sum_{k \in \mathcal{J}} |k|^{2\alpha} |u_k|^2 < \infty, \quad k \cdot u_k = 0 \quad \text{and} \quad u_{-k} = \overline{u_k} \right\}.$$

Here $\mathcal{J} = \{\, 2\pi n/L : n \in \mathbf{Z}^2 \setminus \{0\}\}$ and $u_k \in \mathbf{C}^2$ are the Fourier coefficients for the velocity field $u$. The zero spatial average along with Parseval's identity implies the norms and inner products for the $V_\alpha$ spaces are equivalent to

$$\|u\|_\alpha = \Big(L^2 \sum_{k\in\mathcal{J}} |k|^{2\alpha}|u_k|^2\Big)^{1/2} \qquad \text{and} \qquad ((u,v))_\alpha = L^2 \sum_{k\in\mathcal{J}} |k|^{2\alpha} u_k \overline{v_k}.$$

Recall that $V_\alpha \subseteq V_\beta$ for $\beta \le \alpha$ with corresponding Poincaré inequalities

$$\lambda_1^{\alpha-\beta}\|u\|_\beta^2 \le \|u\|_\alpha^2 \qquad \text{for} \qquad u \in V_\alpha, \tag{2.3}$$

where $\lambda_1 = (2\pi/L)^2$. Denote the norms corresponding to $H$, $V$ and $\mathcal{D}(A)$ by

$$|u| = \|u\|_0, \qquad \|u\| = \|u\|_1 \qquad \text{and} \qquad |Au| = \|u\|_2$$

and the inner products by

$$(u,v) = ((u,v))_0, \qquad ((u,v)) = ((u,v))_1 \qquad \text{and} \qquad (Au,Av) = ((u,v))_2.$$

Along with the above functional notation the following *a priori* bounds also appear in [7], [28] and [29] for the incompressible Navier–Stokes equations:

**Theorem 2.1.** *Let $U$ be a solution to* (2.2) *with $f \in V$ and initial condition $U_0 \in \mathcal{D}(A)$. There exist bounds $\rho_\alpha$ and $\widetilde{\rho}_\alpha$ depending only on $\delta_{\max}$, $\nu$, $\|f\|$ and $U_0$ such that*

$$|A^{\alpha/2}U| \le \rho_\alpha \quad \textit{for} \quad \alpha = 0,1,2 \tag{2.4}$$

*and*

$$\Big(\int_{t_n}^{t_{n+1}} |A^{\alpha/2}U|^2 dt\Big)^{1/2} \le \widetilde{\rho}_\alpha \quad \textit{for} \quad \alpha = 1,2,3. \tag{2.5}$$

*Furthermore,* (2.2) *possesses a unique global attractor $\mathcal{A}$ bounded in $\mathcal{D}(A)$. Moreover, if $U$ lies on that global attractor, then the constants $\rho_\alpha$ and $\widetilde{\rho}_\alpha$ may be taken independent of $U_0$.*

We remark that a well-posed dissipative dynamical system of the form (1.1) may now be obtained by taking $\mathcal{F}(U) = f - B(U,U) - \nu AU$. Let $S$ be the solution operator such that $S(t)U_0 = U(t)$, where $U(t)$ is the unique solution to (2.2) with initial condition $U_0$ at time $t_0 = 0$. Well-posedness along with the fact that the dynamics are autonomous implies $S(t+\delta) = S(\delta)S(t)$ for $t \ge 0$ and $\delta \ge 0$.

The smoothing filter defined in (2.7) can be generalized. Given any $V$ that is compactly and densely embedded in $H$ consider the embedding $\iota\colon V \to H$. By the spectral theorem for compact, self-adjoint operators applied to $\iota^*\iota\colon V \to V$ there exists an orthonormal basis $\phi_k$ of $V$. Assume this basis has been ordered so the eigenvalues $\lambda_k$ are non-increasing. Since $V$ is dense, then $\phi_k$ is also a basis of $H$. Now (2.7) for any $u \in H$ becomes

$$P_\lambda u = \sum_{0<\lambda_k\le\lambda} u_k\phi_k \qquad \text{where} \qquad u = \sum_{k\in\mathcal{J}} u_k\phi_k. \tag{2.6}$$

Clearly, (2.8) and (2.9) still hold. Note for the spaces $V$ and $H$ defined above the eigenfunctions $\phi_k$ turn out to be exactly $e^{ik\cdot x}$.

Thus, the spectral filter considered here and previously in [6] is given for $u \in H$ as

$$P_\lambda u = \sum_{0<|k|^2\le\lambda} u_k e^{ik\cdot x} \qquad \text{where} \qquad u = \sum_{k\in\mathcal{J}} u_k e^{ik\cdot x}. \tag{2.7}$$

Note the interpolation property

$$|u - P_\lambda u|^2 = L^2 \sum_{|k|^2>\lambda} |u_k|^2 \le L^2 \sum_{|k|^2>\lambda} \frac{|k|^2}{\lambda} |u_k|^2 \le \lambda^{-1}\|u\|^2 \quad \text{for} \quad u \in V, \tag{2.8}$$

and the smoothing properties

$$\|P_\lambda u\|_\alpha^2 = L^2 \sum_{0<|k|^2\le\lambda} |k|^{2\alpha}|u_k|^2 \le \lambda^\alpha L^2 \sum_{0<|k|^2\le\lambda} |u_k|^2 \le \lambda^\alpha |u|^2 \quad \text{for} \quad u \in H. \tag{2.9}$$

In particular, note that $\|P_\lambda u\|^2 \le \lambda |u|^2$ and $|AP_\lambda u|^2 \le \lambda^2|u|^2$. Similarly $|AP_\lambda u|^2 \le \lambda \|u\|^2$.

Assume the observations are interpolated back into the phase space of $U$ by a linear operator $I_h\colon V \to L^2(\Omega)$ that satisfies

$$|U - P_H I_h U|^2 \le c_1 h^2 \|U\|^2 \quad \text{for every} \quad U \in V \quad \text{and} \quad h > 0. \tag{2.10}$$

Here $h$ is a length scale that reflects the resolution of the observations. Note (2.10) provides a bound on the relative error in the spirit of the Bramble–Hilbert Lemma and that there is no requirement on $I_h$ or $P_H I_h$ to be a projection. Linearity, however, is important.

The operators $I_h$ were introduced in [2] as type-I interpolant observables and generally result from spatially-averaged observations, for example, the determining volume elements of Jones and Titi [24] and the local spatial averages from Appendix A in [5]. The latter may be seen as an approximation of point measurements, which are classified as type-II observables and rely on higher norms such as $|Au|$ to obtain inequalities similar to (2.10).

Since $P_H I_h$ may not be an orthogonal projection, lack of orthogonality complicates the use of $P_H I_h U$ for data assimilation. Another difficulty is the possible roughness of $I_h$. Such roughness may be characterized as the case when $P_H I_h U \notin V$. This difficulty was mediated in [6] by the use of $P_\lambda$ as a smoothing filter. To this end set

$$J = P_\lambda P_H I_h \tag{2.11}$$

where $P_\lambda$ is the spectral filter (2.7) and consider the smoothed observations given by $JU$.

This results in an interpolant that satisfies

$$|U - JU|^2 = |U - P_\lambda U|^2 + |P_\lambda(U - P_H I_h U)|^2 \le (\lambda^{-1} + c_1 h^2)\|U\|^2 \tag{2.12}$$

and

$$\|U - JU\|^2 = \|U - P_\lambda U\|^2 + \|P_\lambda(U - P_H I_h U)\|^2 \le \big(1 + \lambda c_1 h^2\big)\|U\|^2, \tag{2.13}$$

which has the continuity properties

$$|JU| = |U - JU| + |U| \le (\lambda^{-1} + c_1 h^2)^{1/2}\|U\| + \lambda_1^{-1}\|U\| \le c_2\|U\| \tag{2.14}$$

and

$$\|JU\| = \|U - JU\| + \|U\| \le (1 + \lambda c_1 h^2)^{1/2}\|U\| + \|U\| \le c_3\|U\| \tag{2.15}$$

where $c_2 = (\lambda^{-1} + c_1 h^2)^{1/2} + \lambda_1^{-1/2}$ and $c_3 = (1 + \lambda c_1 h^2)^{1/2} + 1$.

# 3 Numerical Results

Our numerical study begins by taking $\kappa = 1$ to verify that the theoretical constraint from [6] is physical and the skill of the data assimilation algorithm given by Definition 1.1 actually does degrade when taking observations more frequently in time. After this we vary $\kappa$ to determine how the optimal value of $\kappa$ depends on $\delta$ numerically. We then present numerical evidence that taking the relaxation parameter $\kappa$ proportional to $\delta$ results in numerical synchronization of the approximating solution with the reference solution when $0 < \delta \le 0.5$. This provides a numerical confirmation of Conjecture 1.4 with $\delta_0 = 0.5$ that further depends on the particular domain and choice of $f$ and $\nu$ used in our simulations.

All simulations are performed for a $2\pi$-periodic domain discretized on a $512 \times 512$ spatial grid using a dealiased spectral method with 115599 active Fourier modes. Integration in time was by means of the fourth-order exponential time-differencing method introduced by Cox and Matthews [8] with step size $\Delta t = 0.0078125$. To avoid loss of precision the coefficients for the time-stepping method were obtained as in Kassam and Trefethen [25].

The computer program that performs the data assimilation experiments presented in this paper is written in the C programming language by the authors and compiled with GCC [16]. This same code was previously used in [5] to study the effects of noise in time-delay nudging. An overview of how this program works follows. The MPICH MPI library [1] distributes the computation of the reference and corresponding approximating solutions among the computational nodes. Each MPI rank is threaded using OpenMP and the Fourier transforms are performed using the FFTW library of Frigo and Johnson [15]. While running, our simulations compute the reference solution using MPI rank 0 and every $m$ time steps where $m\Delta t = \delta$ send the observational measurements of $U$ to the remaining ranks. Those ranks then construct for different values of $\kappa$ the corresponding approximating solutions.

We remark the one-way flow of observations from rank 0 to the other MPI ranks mimic real-world data gathering. This one-way flow of information also means network communication latency does not significantly affect the performance of our simulations. As a result the data-assimilation experiments could be parallelized across a loosely-coupled cluster of available machines using relatively low-speed gigabit Ethernet.

We now describe further details of the data assimilation experiments. The observational measurements are given by 81 local spatial averages around the points

$$p_i = \big( \lfloor x_{i,1}(256/\pi) + 0.5 \rfloor, \lfloor x_{i,2}(256/\pi) + 0.5 \rfloor \big)$$

on a $512 \times 512$ grid where

$$x_i \in \big\{ \big( (2n_1+1)\pi/9, (2n_2+1)\pi/9 \big) : n_1, n_2 = 0, \ldots, 8 \big\}.$$

The spatial averages are computed as

$$U_i \approx \frac{1}{|\mathcal{B}_i|} \sum_{p \in \mathcal{B}_i} U(p\pi/256) \qquad \text{where} \qquad \mathcal{B}_i = \big\{ p \in \mathbf{Z}^2 : |p - p_i|^2 \le 24 \big\}.$$

The condition $|p - p_i|^2 \le 24$ corresponds to an averaging radius of about $\sqrt{24}\pi/256 \approx 0.06$ in the $2\pi$-periodic domain. Note there are $|\mathcal{B}_i| = 69$ grid points in each average. Since the

Figure 1: The error $|U(t)-u(t)|$ for a reference solution $U(t)$ where the approximating solution $u(t)$ was computed for different observation intervals $\delta$. Large $\delta$ is shown on the left; small on the right.

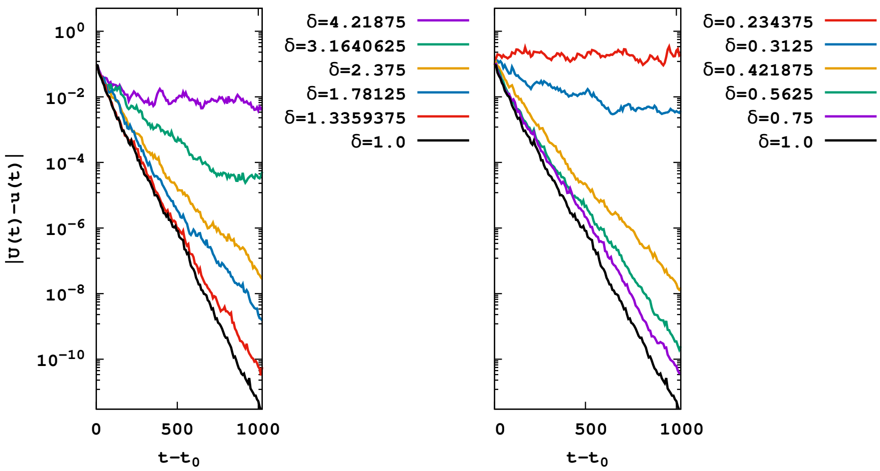


Figure 2: The same calculation as Figure 1 redone for a different reference solution $U(t)$ lying on the global attractor.

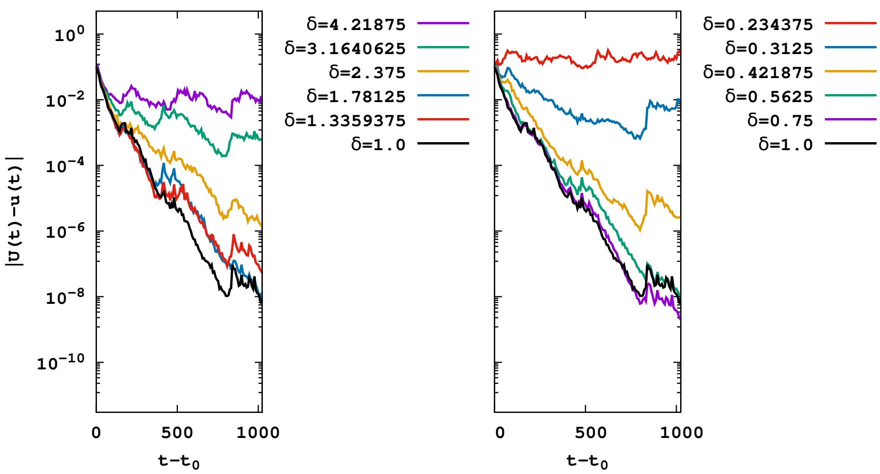


grid consists of $512^2 = 262144$ points total, the local averages cover about 2.13 percent of the physical domain. This percentage may be interpreted as how well the spatial averages reflect point observations of the velocity fields.

As the MPI ranks used for computing an approximating solution receive the observational data it is interpolated as

$$JU(p) = P_\lambda P_H \sum_{i=1}^{81} U_i \chi_i(p)$$

where $\chi_i$ is the characteristic function for the square centered at $p_i$.

We begin by presenting numerical evidence to illustrate the constraints on the observation frequency when using the original spectrally-filtered discrete-in-time method for data assimilation. Consider a fixed trajectory $U(t)$ on the global attractor of the two-dimensional Navier–Stokes equations obtained by a long-time integration of (2.2) forward in time. Next, apply Definition 1.1 to compute $u(t)$ for different values of $\delta$ while holding all other parameters and the trajectory $U(t)$ fixed.

The evolutions of $|U(t) - u(t)|$ for the resulting simulations are depicted in Figure 1. Consider the value of $|U(T) - u(T)|$ at $T = t_0 + 1024$ for the different values of $\delta$ and the behavior of each curve leading up to that time. The graph on the left suggests $|U(t) - u(t)|$ does not tend to zero as $t \to \infty$ for values of $\delta$ where $\delta > 3$. More surprisingly the graph on the right suggests $|U(t) - u(t)|$ does not tend to zero when $\delta < 0.3$. Thus, taking $\delta$ either too small or too large results in failure of the approximating solution $u$ to synchronize with $U$. This is consistent with the commentary associated with the proof of Theorem 1.3.

Note the skill by which Definition 1.1 recovers the reference solution $U(t)$ depends on the specific trajectory being observed. Some reference solutions may exhibit dynamical behaviors that are more difficult to recover from the observational data while others are easier to recover. Figure 2 repeats the calculations of Figure 1 for a different reference solution on the global attractor. While the size of $|U(T) - u(T)|$ at $T = t_0 + 1024$ is four decimal orders of magnitude larger in Figure 2 compared to Figure 1, the trends of the curves for large and small values of $\delta$ are similar. In particular, taking $\delta$ either too small or too large results in failure of the approximating solution $u$ to synchronize with $U$ in both cases while $\delta \approx 1$ is a good choice for the observation interval.

Figure 3: The ensemble average and geometric mean compared to box plots (no outliers removed) of the error $|U(T) - u(T)|$ at time $T = t_0 + 1024$ for 500 simulations varying $\delta$.

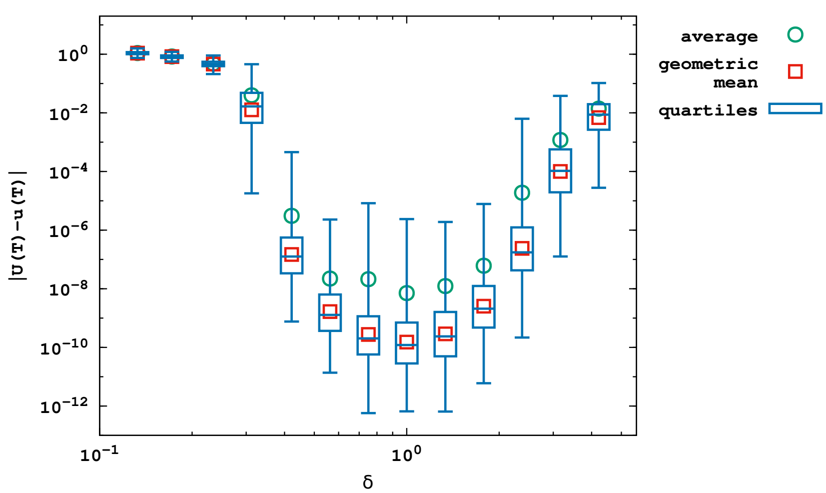


To further characterize the rate at which the approximating solution converges to the reference solution for different values of $\delta$, the experiments of Figures 1 and 2 were repeated for an ensemble of 500 reference solutions randomly chosen on the global attractor. Let $\mathcal{E}$ be a fixed ensemble. Compute the ensemble average error for each $\delta$ as

$$\langle |U(T) - u(T)| \rangle = \frac{1}{|\mathcal{E}|} \sum_{U \in \mathcal{E}} |U(T) - u(T)|$$

and the geometric mean as

$$\mathrm{GM}\big[|U(T)-u(T)|\big] = \exp\Big(\frac{1}{|\mathcal{E}|}\sum_{U\in\mathcal{E}} \log|U(T)-u(T)|\Big).$$

Here $|\mathcal{E}|$ is the number of solutions in the ensemble.

The ensemble $\mathcal{E}$ was obtained from the long-term evolutions of randomly-chosen points in phase space. In particular $U \in \mathcal{E}$ implies $U(t_0) = U_0$ where $U_0 = S(10240)Z_0$ and $Z_0$ is a random velocity field with energy spectrum similar to a point on the attractor. Although $Z_0$ is unlikely to be on the global attractor, the evolution time of 10240 is long enough that large scale structures have appeared in the velocity field and further undergone more than 300 large eddy turnovers. We remark that the energetics of each flow appear to enter into a statistically-steady state while continuing to undergo complex fluctuations. This suggests the initial conditions $U_0$ for each of the trajectories in $\mathcal{E}$ lie very near the global attractor and that this attractor is nontrivial.

Figure 3 reports the ensemble averages corresponding to $\delta \in [0.1328125, 4.21875]$ along with the median and some additional statistics. The whiskers in the box plots are long because no outliers have been removed. We remark the ensemble average lies above the median because it is dominated by the few trajectories in $\mathcal{E}$ that lead to errors at time $T$ with large magnitudes similar to Figure 2 while the geometric mean and median are much closer. Since the median and geometric mean are more robust in the presence of extreme variations, the $\delta$ which minimizes the error shall be identified using these statistics. In particular, note that $\delta \approx 1$ minimizes the geometric mean of the error.

We now consider the $\kappa$-relaxed data assimilation method given by Definition 1.2 that is the main focus of our research. To identify the relationship between $\kappa$ and $\delta$ we performed additional data-assimilation experiments for sampling intervals of

$$\delta = m\Delta t \qquad \text{where} \qquad m = \Big\lfloor 228\Big(\frac{3}{4}\Big)^p \Big\rfloor \qquad \text{for} \qquad p = 0, 1, \ldots, 17 \tag{3.1}$$

and the relaxation parameters

$$\kappa = \Big(\frac{3}{4}\Big)^{q/3} \qquad \text{for which} \qquad \kappa \in \big[0.0056, 5\delta\big] \qquad \text{and} \qquad q \in \mathbf{Z}. \tag{3.2}$$

In all we consider 873 choices for $\delta$ and $\kappa$. For each choice multiple simulations were performed corresponding to the ensemble $\mathcal{E}$ of 500 different reference solutions identified earlier. This resulted in a total of 436500 data assimilation experiments.

We note the available hardware—mostly Xeon and Epyc servers—typically performed from 10 to 30 time steps per second depending on the exact processor and memory speed. To facilitate scheduling, the runs were partitioned into batches that computed the reference solution and corresponding approximating solutions for seven parameter choices at a time. For each choice of parameters the final value of $|U(T) - \tilde{u}(T)|$ at $T = t_0 + 1024$ is returned after 131072 time steps. On average each run about took two hours.

Figure 4 plots the geometric mean of the error at time $T$ for each $\delta \in [0.0078125, 1.78125]$ as a function of $\kappa$ where $\kappa \in [0.0056, 5\delta]$. Note that additional runs when $\delta = 0.0078125$ were performed with $\kappa \in \big[0.00317, 0.0056\big)$ to ensure that small enough values of $\kappa$ were considered for this smallest value of $\delta$.

Figure 4: The geometric mean of $\|U(T) - \tilde{u}(T)\|_{L^2}$ at $T = t_0 + 1024$ for varying values of $\delta$ and $\kappa$.

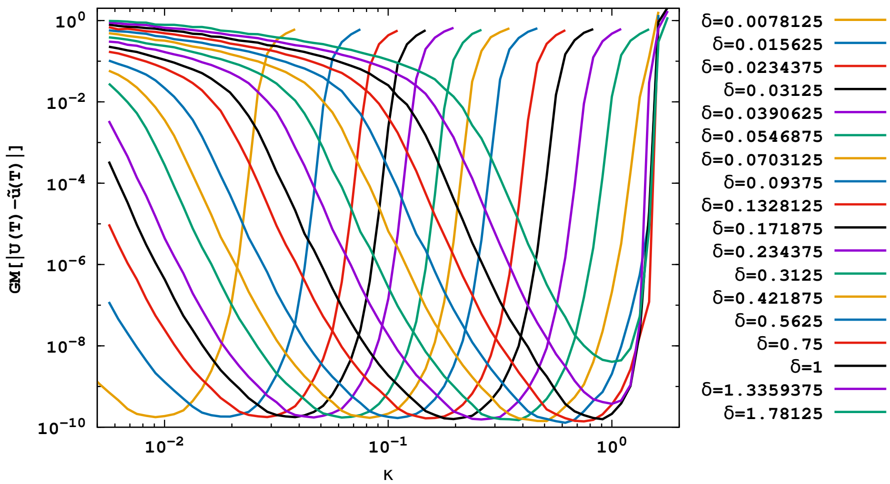


Figure 5: Box plots (no outliers removed) depicting the values of $\kappa$ that minimize $\|U(T)-\tilde{u}(T)\|_{L^2}$ when $T = t_0+1024$ for each trajectory in the ensemble. Note $\kappa = \mu\delta$ was fitted for $\delta \leq 0.5$.

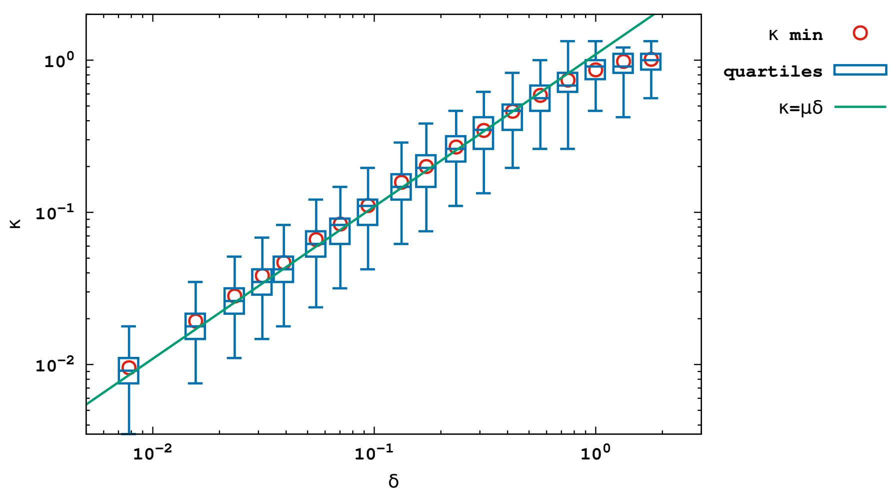


The value $\kappa_{\min}$ of $\kappa$ that minimizes the geometric mean along the corresponding curve for each $\delta$ in Figure 4 was obtained using a least-squares quadratic fit of points near the minimum. To illustrate how $\kappa_{\min}$ depends on $\delta$ the points $(\delta, \kappa_{\min})$ are plotted in Figure 5 as circles. Note for $\delta \leq 0.5$ the relationship between $\kappa_{\min}$ and $\delta$ appears linear. This linearity is our primary numerical result and the focus of the theory in the following section.

Figure 5 further characterizes the relationship between $\kappa$ and $\delta$ by considering each reference trajectory $U \in \mathcal{E}$ separately to obtain 500 different minimizing values of $\kappa$ for each $\delta$. The distribution of the minimizing values of $\kappa$ are then displayed in quartiles for each value of $\delta$ considered. Finally a least squares fit of $\kappa = \mu\delta$ for $\delta \leq 0.5$ was performed to obtain $\mu \approx 0.966$. We remark $\mu$ is not universal but a tuning parameter that depends on the viscosity $\nu$, body forcing $f$, spatial domain and the interpolant observable $J$ among others. In particular, the value of $\mu$ obtained above is only coincidentally close to one. What is important is that the relationship between $\kappa$ and $\delta$ appears linear.

# 4 Theoretical Results

In this section we prove our main theoretical result given as Theorem 1.5 in the introduction. Begin by translating the *a priori* bounds of Theorem 2.1 into bounds on the interpolated observations represented by $JU$.

**Proposition 4.1.** *Suppose $U$ lies on the global attractor of* (2.2) *and $f \in V$. There exists constants $\rho_J$ and $\rho_K$ depending on $\lambda$, $\nu$, $\|f\|$ and $h$ such that*

$$|JU| \le \rho_J \qquad \text{and} \qquad \|JU\| \le \rho_K. \tag{4.1}$$

*Proof.* Estimate using (2.12) followed by (2.4) as

$$|JU| = |U - JU| + |U| \le (\lambda^{-1} + c_1 h^2)^{1/2}\|U\| + |U|$$

to obtain $\rho_J = (\lambda^{-1} + c_1 h^2)^{1/2}\rho_1 + \rho_0$. Similarly use (2.13) to estimate

$$\|JU\| = \|U - JU\| + \|U\| \le (1 + \lambda c_1 h^2)^{1/2}\|U\| + \|U\|.$$

Thus, $\rho_K = (1 + \lambda c_1 h^2)^{1/2}\rho_1 + \rho_1$. □

Our estimates make use of the following version of Theorem 5 from [2] that removes the condition on $h$ and $\mu$ but applies only on a finite time interval $[t_0, T]$.

**Theorem 4.2.** *Suppose $f \in V$ and $v_0 \in \mathcal{D}(A)$. Let $v$ be the solution obtained from* (1.3)*. There exists bounds $R_\alpha$ and $\widetilde{R}_\alpha$ depending on $T$, $t_0$, $\nu$, $\|f\|$ and $v_0$ such that*

$$\|v\|_\alpha \le R_\alpha \qquad \textit{for} \qquad t \in [t_0, T] \qquad \textit{with} \qquad \alpha = 0, 1, 2 \tag{4.2}$$

*and*

$$\Big(\int_{t_n}^{t_{n+1}} \|v\|_\alpha^2 dt\Big)^{1/2} \le \widetilde{R}_\alpha \quad \textit{for} \quad [t_n, t_{n+1}] \subseteq [t_0, T] \quad \textit{with} \quad \alpha = 1, 2, 3. \tag{4.3}$$

The above result follows by adapting the methods used to prove Theorem 5 in [2] to obtain explicit bounds on $v$ that avoid imposing additional conditions on $h$ and $\mu$ but hold only for a finite time interval $[t_0, T]$. We omit the details here but note that the smoothness of both $J$ and $f$ constrain the regularity of $v$.

We remark that $v_0 = u_0$ in (1.3) where $u_0 = JU(t_0)$. Since $J = P_\lambda P_H I_h$ then $P_\lambda v_0 = v_0$. Consequently (2.9) followed by Proposition 4.1 yields the bound

$$|Av_0| = \|P_\lambda v_0\|_2 \le \lambda |v_0| = \lambda |JU(t_0)| \le \lambda \rho_J.$$

In particular, we may assume $v_0 \in \mathcal{D}(A)$ in the proof of Theorem 1.5. Moreover, since the reference solution $U$ lies on the global attractor $\mathcal{A}$ we may further assume the bounds $R_\alpha$ and $\widetilde{R}_\alpha$ to be independent of $U_0$.

Now use (2.12) and (2.13) as in the proof of Proposition 4.1 to obtain bounds on $|Jv|$ and $\|Jv\|$. Thus, there exists $R_J$ and $R_K$ further depending on $h$ and $\lambda$ such that

$$|Jv| \le R_J \qquad \text{and} \qquad \|Jv\| \le R_K. \tag{4.4}$$

A number of inequalities involving the non-linear term are summarized in Chapter II Appendix A of Foias, Manley, Rosa and Temam [13]. We recall here for reference

$$|(B(u,v),w)| \le c|u|^{1/2}\|u\|^{1/2}\|v\|^{1/2}|Av|^{1/2}|w| \tag{4.5}$$

for $u \in V$, $v \in \mathcal{D}(A)$ and $w \in H$ as well as

$$|(B(u,v),w)| \le c|u|^{1/2}|Au|^{1/2}\|v\||w| \tag{4.6}$$

for $u \in \mathcal{D}(A)$, $v \in V$ and $w \in H$. Note that the above inequalities hold for a suitable constant $c$ depending on the domain $\Omega$ which in our case is $L$-periodic.

It follows from (4.5) that

$$|B(u,v)| \le c|u|^{1/2}\|u\|^{1/2}\|v\|^{1/2}|Av|^{1/2} \qquad \text{for} \qquad u \in V \text{ and } v \in \mathcal{D}(A) \tag{4.7}$$

and from (4.6) that

$$|B(u,v)| \le c|u|^{1/2}|Au|^{1/2}\|v\| \qquad \text{for} \qquad u \in \mathcal{D}(A) \text{ and } v \in V. \tag{4.8}$$

Again from (4.7) it follows that

$$\|B(u,v)\| \le c\|u\|^{1/2}|Au|^{1/2}\|v\|^{1/2}|Av|^{1/2} + c|u|^{1/2}\|u\|^{1/2}|Av|^{1/2}|A^{3/2}v|^{1/2} \tag{4.9}$$

for $u \in \mathcal{D}(A)$ and $v \in \mathcal{D}(A^{3/2})$. Setting $u = v$ and interpolating then yields

$$\|B(u,u)\| \le c|u|^{1/2}\|u\|^{1/2}|Au|^{1/2}|A^{3/2}u|^{1/2} \qquad \text{for} \qquad u \in \mathcal{D}(A^{3/2}). \tag{4.10}$$

For simplicity the $c$ appearing above and in (4.11) below will denote a single constant chosen suitably large so all of the inequalities hold.

We shall also employ an estimate appearing in [5], Foias, Mondaini and Titi [14] and Titi [30] based on the Brezis–Gallouët inequality which we state here as

**Proposition 4.3.** *If $v$ and $w$ are in $\mathcal{D}(A)$ then*

$$\big|\big(B(w,v)+B(v,w),Aw\big)\big| \le c\|w\|\|v\|\bigg(1+\log\frac{|Av|}{\lambda_1^{1/2}\|v\|}\bigg)^{1/2}|Aw|, \tag{4.11}$$

*where $c$ is a non-dimensional constant depending only on the domain.*

Fix $T > t_0$. To study the limit on the interval $[t_0,T]$ as the time between observations $\delta \to 0$ define $t_n = t_0 + \delta n$ for $n = 0,\ldots,N$ where $N$ is the greatest integer such that $t_N \le T$. Assume $\delta \le \delta_{\max}$ where $\delta_{\max} \le T - t_0$; otherwise, if $\delta > T - t_0$, then no observations would occur during the interval $[t_0,T]$ and there would be no data to assimilate.

Assume $\delta \le T - t_0$ and define $t_n = t_0 + \delta n$ for $n = 0, \ldots, N$ where $N$ is the greatest integer such that $t_N \le T$. Upon substituting $\kappa = \delta\mu$ into (1.2) the approximating solution $\tilde{u}(t)$ given by Definition 1.2 satisfies

$$\tilde{u}(t) = \begin{cases} S(t - t_n)\tilde{u}_n & \text{for} \quad t \in [t_n, t_{n+1}) \quad \text{with} \quad n = 0, \ldots, N-1, \\ S(t - t_N)\tilde{u}_N & \text{for} \quad t \in [t_N, T] \end{cases}$$

where

$$\begin{cases} \quad \tilde{u}_0 = JU(t_0), \\ \tilde{u}_{n+1} = S(\delta)\tilde{u}_n + \delta\mu J\big\{U(t_{n+1}) - S(\delta)\tilde{u}_n\big\}. \end{cases}$$

In preparation to prove Theorem 1.5 let $w_n = v(t_n) - \tilde{u}_n$ and $w(t) = v(t) - \tilde{u}(t)$. Here $v(t)$ is the continuous-nudging approximation given by (1.3). Note that by definition

$$\tilde{u}(t_{n+1}^-) = \lim_{t \nearrow t_{n+1}} \tilde{u}(t) = S(\delta)\tilde{u}_n.$$

Therefore,

$$\begin{aligned} w_{n+1} &= v(t_{n+1}) - (1 - \delta\mu J)\tilde{u}(t_{n+1}^-) - \delta\mu J U(t_{n+1}) \\ &= w(t_{n+1}^-) - \delta\mu J(U(t_{n+1}) - v(t_{n+1}) + w(t_{n+1}^-)) \\ &= (I - \delta\mu J)w(t_{n+1}^-) - \delta\mu J(U(t_{n+1}) - v(t_{n+1})). \end{aligned}$$

Consequently $w$ satisfies

$$\frac{dw}{dt} + \nu A w + B(v, w) + B(w, v) - B(w, w) = \mu J(U - v) \quad \text{on} \quad t \in [t_n, t_{n+1}) \tag{4.12}$$

with initial condition

$$w_n = (I - \delta\mu J)w(t_n^-) - \delta\mu J(U(t_n) - v(t_n)) \qquad \text{for} \qquad n > 0 \tag{4.13}$$

and $w_0 = 0$ since we use the same initial state for both data assimilation methods. For notational convenience we define $w(t_0^-) = 0$ so that (4.13) also holds when $n = 0$.

Continue with the following estimate on the integral of $L^2$ norm of $Aw$.

**Theorem 4.4.** *There exists $M_0$, $M_1$ and $\widetilde{M}_2$ depending only on $T$, $t_0$, $\nu$, $\|f\|$ and the domain $\Omega$ such that*

$$|w| \le M_0 \qquad \text{and} \qquad \|w\| \le M_1 \qquad \text{for all} \qquad t \in [t_0, T]$$

*and*

$$\Big(\int_{t_n}^{t_{n+1}} |Aw|^2 dt\Big)^{1/2} \le \widetilde{M}_2 \qquad \text{for} \qquad [t_n, t_{n+1}] \subseteq [t_0, T]. \tag{4.14}$$

*Proof.* Let $N$ be the greatest integer such that $t_N \le T$. By Theorem 4.2 there exists $R_\alpha$ such that $\|v\|_\alpha \le R_\alpha$ for $t \in [t_0, T]$ and $\alpha = 0, 1, 2$. Since the reference trajectory $U$ lies on the global attractor and $v_0 = JU(t_0)$ than these bounds can be taken independent of $v_0$. Multiply (4.12) by $Aw$ and use the fact that $(B(w, w), Aw) = 0$ in two-dimensional periodic domains to obtain

$$\frac{1}{2}\frac{d\|w\|^2}{dt} + \nu|Aw|^2 + (B(v, w), Aw) + (B(w, v), Aw) = \mu(J(U - v), Aw). \tag{4.15}$$

From (4.11) it follows that

$$
\begin{aligned}
|(B(v,w),Aw)+(B(w,v),Aw)| &\le c\|w\|\|v\|\left(1+\log\frac{|Av|}{\lambda_1^{1/2}\|v\|}\right)^{1/2}|Aw| \\
&\le cR_1^{1/2}R_L^{1/2}\|w\||Aw| \le \frac{c^2R_1R_L}{\nu}\|w\|^2+\frac{\nu}{4}|Aw|^2, \qquad (4.16)
\end{aligned}
$$

where

$$
R_L = R_1\left(1+\log\frac{R_2}{\lambda_1^{1/2}R_1}\right).
$$

Also

$$
\mu(J(U-v),Aw) \le \frac{\mu^2}{\nu}|J(U-v)|^2+\frac{\nu}{4}|Aw|^2 \le \frac{\mu^2}{\nu}C_1^2+\frac{\nu}{4}|Aw|^2 \qquad (4.17)
$$

where $C_1=\rho_J+R_J$.

Combining (4.16) and (4.17) with (4.15) yields

$$
\frac{d\|w\|^2}{dt}+\nu|Aw|^2 \le \frac{2c^2R_1R_L}{\nu}\|w\|^2+\frac{2\mu^2}{\nu}C_1^2 \le C_2\|w\|^2+C_3. \qquad (4.18)
$$

Here $C_2=2c^2R_1R_L/\nu$ and $C_3=2\mu^2C_1^2/\nu$. Now multiply (4.18) by $e^{-C_2t}$ and integrate from $t_n$ to $t$ where $t\in[t_n,t_{n+1})$ for $n=0,1,\dots,N-1$ and $t\in[t_N,T]$ for $n=N$. Thus,

$$
\|w(t)\|^2+\nu\int_{t_n}^t e^{C_2(t-s)}|Aw(s)|^2ds \le e^{C_2(t-t_n)}\|w_n\|^2+\frac{C_3}{C_2}\big(e^{C_2(t-t_n)}-1\big). \qquad (4.19)
$$

We obtain after applying (2.13) that

$$
\begin{aligned}
\|w_n\| &= \|(I-\delta\mu J)w(t_n^-)-\delta\mu J(U(t_n)-v(t_n))\| \\
&\le |1-\delta\mu|\|w(t_n^-)\|+\delta\mu\|(I-J)w(t_n^-)\|+\delta\mu\|J(U(t_n)-v(t_n))\|.
\end{aligned}
$$

Therefore

$$
\|w_n\| \le (1+\delta\mu C_4)\|w(t_n^-)\|+\delta\mu C_5 \qquad (4.20)
$$

where $C_4=1+\sqrt{1+\lambda c_1h^2}$ and $C_5=\rho_K+R_K$. Consequently, under the assumption $\delta\le\delta_{\max}$ it follows that

$$
\begin{aligned}
\|w_n\|^2 &\le (1+\delta\mu C_4)^2\|w(t_n^-)\|^2+2\delta\mu(1+\delta\mu C_4)C_5\|w(t_n^-)\|+\delta^2\mu^2C_5^2 \\
&\le (1+\delta\mu C_4)^2\|w(t_n^-)\|^2+\delta\mu\big\{(1+\delta\mu C_4)^2\|w(t_n^-)\|^2+C_5^2\big\}+\delta^2\mu^2C_5^2 \\
&= (1+\delta\mu)(1+\delta\mu C_4)^2\|w(t_n^-)\|^2+\delta\mu(1+\delta\mu)C_5^2 \\
&\le (1+\delta\mu C_6)\|w(t_n^-)\|^2+\delta\mu C_7
\end{aligned}
$$

where $C_6=2C_4+\delta_{\max}\mu C_4^2+(1+\delta_{\max}\mu C_4)^2$ and $C_7=(1+\delta_{\max}\mu)C_5^2$.

Substituting into (4.19) and dropping the integral on the left results in

$$
\|w(t)\|^2 \le e^{C_2(t-t_n)}\big\{(1+\delta\mu C_6)\|w(t_n^-)\|^2+\delta\mu C_7\big\}+\frac{C_3}{C_2}\big(e^{C_2(t-t_n)}-1\big). \qquad (4.21)
$$

Subsequently for $n = 0, 1, \ldots, N-1$ taking the limit as $t \to t_{n+1}$ obtains

$$\|w(t_{n+1}^-)\|^2 \le e^{\delta C_2}(1+\delta\mu C_6)\|w(t_n^-)\|^2 + \delta\mu e^{\delta C_2} C_7 + \frac{C_3}{C_2}\big(e^{\delta C_2} - 1\big).$$

Setting $y_n = \|w(t_n^-)\|^2$ gives the inequality $y_{n+1} \le \alpha y_n + \beta$ where $\alpha = e^{\delta C_2}(1+\delta\mu C_6)$ and $\beta = \delta\mu e^{\delta C_2} C_7 + (C_3/C_2)(e^{\delta C_2} - 1)$. By induction

$$\begin{aligned}
&y_1 \le \alpha y_0 + \beta \\
&y_2 \le \alpha y_1 + \beta \le \alpha^2 y_0 + (1+\alpha)\beta \\
&\quad\vdots \\
&y_n \le \alpha^n y_0 + \textstyle\sum_{j=0}^{n-1} \alpha^j \beta \le \alpha^n y_0 + \frac{\alpha^n - 1}{\alpha - 1}\beta.
\end{aligned}$$

Using the fact that $x \le e^x - 1 \le x e^x$ for $x \ge 0$ we obtain

$$\alpha - 1 = e^{\delta C_2} - 1 + \delta\mu e^{\delta C_2} C_6 \ge \delta(C_2 + \mu e^{\delta C_2} C_6),$$

$$\alpha^n = e^{n\delta C_2}(1+\delta\mu C_6)^n \le e^{(t_n - t_0)(C_2 + \mu C_6)}$$

and

$$\beta = \delta\mu e^{\delta C_2} C_7 + (C_3/C_2)(e^{\delta C_2} - 1) \le \delta e^{\delta C_2}(\mu C_7 + C_3).$$

Consequently, for $n = 1, 2, \ldots, N$ it follows from $\delta \le \delta_{\max}$ that

$$\begin{aligned}
\|w(t_n^-)\|^2 &\le e^{(t_n - t_0)(C_2+\mu C_6)}\|w(t_0^-)\|^2 + \frac{e^{(t_n - t_0)(C_2+\mu C_6)} - 1}{C_2 + \mu e^{\delta C_2} C_6} e^{\delta C_2}(\mu C_7 + C_3) \\
&\le e^{2\delta_{\max}(C_2+\mu C_6)}\|w(t_0^-)\|^2 + \frac{e^{2\delta_{\max}(C_2+\mu C_6)} - 1}{(C_2 + \mu C_6)} e^{\delta_{\max} C_2}(\mu C_7 + C_3).
\end{aligned}$$

Since $\|w(t_0^-)\| = 0$, there is a constant $C_8$ independent of $\delta$ such that

$$\|w(t_n^-)\| \le C_8 \qquad \text{for} \qquad n = 1, \ldots, N.$$

It follows from (4.20) that

$$\|w_n\| \le (1+\delta\mu C_4)\|w(t_n^-)\| + \delta\mu C_5 \le (1+\delta_{\max}\mu C_4)C_8 + \delta_{\max}\mu C_5$$

and so there is also a constant $C_9$ independent of $\delta$ such that

$$\|w_n\| \le C_9 \qquad \text{for} \qquad n = 1, \ldots, N.$$

Now use (4.19) to show there is $M_1$ such that $\|w(t)\| \le M_1$ for $t \in [t_0, T]$. Note that

$$M_1^2 = e^{C_2\delta_{\max}} C_9^2 + \frac{C_3}{C_2}\big(e^{C_2\delta_{\max}} - 1\big).$$

The Poincaré inequality (2.3) stated as $\lambda_1 |w|^2 \le \|w\|^2$ immediately implies

$$|w(t)| \le \lambda_1^{-1/2}\|w(t)\| \le M_0 \qquad \text{for} \qquad t \in [t_0, T]$$

where $M_0 = \lambda_1^{-1/2} M_1$.

To obtain (4.14) suppose $n = 0, 1, \ldots, N-1$ and integrate (4.18) from $t_n$ to $t$. Then taking the limit as $t \to t_{n+1}$ yields

$$\|w(t_{n+1}^-)\|^2 - \|w_n\|^2 + \nu \int_{t_n}^{t_{n+1}} |Aw|^2 dt \le C_2 \int_{t_n}^{t_{n+1}} \|w\|^2 dt + \delta C_3.$$

Thus

$$\nu \int_{t_n}^{t_{n+1}} |Aw|^2 dt \le \|w_n\|^2 + \delta_{\max}(C_2 M_1^2 + C_3)$$

or equivalently

$$\Big( \int_{t_n}^{t_{n+1}} |Aw|^2 dt \Big)^{1/2} \le \widetilde{M}_2 \qquad \text{where} \qquad \widetilde{M}_2^2 = \frac{C_9^2}{\nu} + \delta_{\max} \frac{C_2 M_1^2 + C_3}{\nu}.$$

Finally, noting that $M_0$, $M_1$ and $\widetilde{M}_2$ depend only on $T$, $t_0$, $\nu$, $\|f\|$ and $\Omega$ finishes the proof. □

**Corollary 4.5.** *There exists constants $M_J$ and $M_K$ such that*

$$|Jw| \le M_J \qquad \textit{and} \qquad \|Jw\| \le M_K \qquad \textit{for all} \qquad t \in [t_0, T].$$

*Proof.* This follows at once from Theorem 4.4 applied to (2.12) and (2.13) exactly analogous to the way (4.1) and (4.4) were obtained. □

The next step is to bootstrap Theorem 4.4 to obtain bounds which tend to zero as $\delta \to 0$. In order to do this we first prove the following two lemmas.

**Lemma 4.6.** *There exists $M_D$ independent of $\delta$ such that*

$$\int_{t_n}^{t_{n+1}} |w(t) - w_n| dt \le \delta^{3/2} M_D \qquad \textit{for} \qquad [t_n, t_{n+1}] \subseteq [t_0, T].$$

*Proof.* Estimate as

$$\begin{aligned}\int_{t_n}^{t_{n+1}} |w(t) - w_n| dt &\le \int_{t_n}^{t_{n+1}} \int_{t_n}^{s} \Big| \frac{dw(t)}{dt} \Big| dt\, ds \le \delta \int_{t_n}^{t_{n+1}} \Big| \frac{dw(t)}{dt} \Big| dt \\ &\le \delta \int_{t_n}^{t_{n+1}} \big\{ \nu |Aw| + |B(v,w)| + |B(w,v)| + |B(w,w)| + \mu |J(U-v)| \big\}.\end{aligned}$$

By the Theorem 4.4 we have

$$\int_{t_n}^{t_{n+1}} \nu |Aw| \le \nu \delta^{1/2} \Big( \int_{t_n}^{t_{n+1}} |Aw|^2 \Big)^{1/2} \le \delta^{1/2} \nu \widetilde{M}_2. \tag{4.22}$$

Using (4.7) we have

$$\begin{aligned}\int_{t_n}^{t_{n+1}} |B(v,w)| &\le c \int_{t_n}^{t_{n+1}} |v|^{1/2} \|v\|^{1/2} \|w\|^{1/2} |Aw|^{1/2} \le c R_0^{1/2} R_1^{1/2} M_1^{1/2} \int_{t_n}^{t_{n+1}} |Aw|^{1/2} \\ &\le c R_0^{1/2} R_1^{1/2} M_1^{1/2} \delta^{3/4} \Big( \int_{t_n}^{t_{n+1}} |Aw|^2 \Big)^{1/4} \le \delta^{3/4} c R_0^{1/2} R_1^{1/2} M_1^{1/2} \widetilde{M}_2^{1/2}\end{aligned}$$

and from (4.8) it follows

$$\int_{t_n}^{t_{n+1}} |B(w,v)| \le c \int_{t_n}^{t_{n+1}} |w|^{1/2}|Aw|^{1/2}\|v\| \le \delta^{3/4} c M_0^{1/2} R_1 \widetilde{M}_2^{1/2}.$$

as well as

$$\int_{t_n}^{t_{n+1}} |B(w,w)| \le c \int_{t_n}^{t_{n+1}} |w|^{1/2}|Aw|^{1/2}\|w\| \le \delta^{3/4} c M_0^{1/2} M_1 \widetilde{M}_2^{1/2}.$$

Finally,

$$\int_{t_n}^{t_{n+1}} \mu|J(U-v)| \le \delta\mu(\rho_J + R_J).$$

Upon collecting the above estimates together we obtain

$$\int_{t_n}^{t_{n+1}} |w(t) - w_n| dt \le \delta^{3/2} M_D$$

where

$$M_D = \nu\widetilde{M}_2 + \delta_{\max}^{1/4} c\big\{R_0^{1/2} R_1^{1/2} M_1^{1/2} + M_0^{1/2} R_1 + M_0^{1/2} M_1\big\}\widetilde{M}_2^{1/2} + \delta_{\max}^{1/2}\mu(\rho_J + R_J).$$

Noting that $M_D$ is independent of $\delta$ finishes the proof. □

**Corollary 4.7.** *There exists $M_E$ independent of $\delta$ such that*

$$\int_{t_n}^{t_{n+1}} |w(t) - w(t_n^-)| dt \le \delta^{3/2} M_E \qquad \textit{for} \qquad [t_n, t_{n+1}] \subseteq [t_0, T].$$

*Proof.* Since $w_n - w(t_n^-) = -\delta\mu J\big(w(t_n^-) + U(t_n) - v(t_n)\big)$ then

$$\int_{t_n}^{t_{n+1}} |w_n - w(t_n^-)| dt \le \delta^2\mu(M_J + \rho_J + R_J).$$

It follows from Lemma 4.6 that

$$\int_{t_n}^{t_{n+1}} |w(t) - w(t_n^-)| dt \le \delta^{3/2} M_D + \delta^2\mu(M_J + \rho_J + R_J) \le \delta^{3/2} M_E$$

where $M_E = M_D + \delta_{\max}^{1/2}\mu(M_J + \rho_J + R_J)$. □

**Lemma 4.8.** *There exists $\rho_D$ and $R_D$ independent of $\delta$ such that for $[t_n, t_{n+1}] \subseteq [t_0, T]$ holds*

$$\int_{t_n}^{t_{n+1}} \|J(U(t) - U(t_n))\| dt \le \delta^{3/2}\rho_D \quad \textit{and} \quad \int_{t_n}^{t_{n+1}} \|J(v(t) - v(t_n))\| dt \le \delta^{3/2} R_D.$$

*Proof.* Estimate using (2.15)

$$\int_{t_n}^{t_{n+1}} \|J(U(t)-U(t_n))\|dt \le c_3 \int_{t_n}^{t_{n+1}} \|U(t)-U(t_n)\|dt \le c_3 \int_{t_n}^{t_{n+1}} \int_{t_n}^{s} \Big\|\frac{dU(t)}{dt}\Big\| dt\, ds$$
$$\le c_3\delta \int_{t_n}^{t_{n+1}} \big\{\nu\|AU\| + \|B(U,U)\| + \|f\|\big\}$$

By the Cauchy–Schwartz inequality and (2.5)

$$\nu \int_{t_n}^{t_{n+1}} \|AU\| \le \delta^{1/2}\nu\Big(\int_{t_n}^{t_{n+1}} \|AU\|^2\Big)^{1/2} \le \delta^{1/2}\nu\widetilde{\rho}_3.$$

Similarly (4.10) implies

$$\int_{t_n}^{t_{n+1}} \|B(U,U)\| \le c\int_{t_n}^{t_{n+1}} |U|^{1/2}\|U\|^{1/2}|AU|^{1/2}|A^{3/2}U|^{1/2}$$
$$\le c\int_{t_n}^{t_{n+1}} \rho_0^{1/2}\rho_1^{1/2}|AU|^{1/2}|A^{3/2}U|^{1/2} \le \delta^{1/2}c(\rho_0\rho_1\widetilde{\rho}_2\widetilde{\rho}_3)^{1/2}.$$

Therefore,

$$\rho_D = c_3\big(\nu\widetilde{\rho}_3 + c(\rho_0\rho_1\widetilde{\rho}_2\widetilde{\rho}_3)^{1/2} + \delta_{\max}^{1/2}\|f\|\big).$$

The proof of the second inequality is similar except there is one more term which we estimate using (4.1) and (4.4) as

$$\int_{t_n}^{t_{n+1}} \|J(v(t)-v(t_n))\|dt \le c_3 \int_{t_n}^{t_{n+1}} \|v(t)-v(t_n)\|dt \le c_3 \int_{t_n}^{t_{n+1}} \int_{t_n}^{s} \Big\|\frac{dv(t)}{dt}\Big\| dt\, ds$$
$$\le c_3\delta \int_{t_n}^{t_{n+1}} \big\{\nu\|Av\| + \|B(v,v)\| + \|f\| + \mu\|J(U-v)\|\big\} \le \delta^{3/2}R_D$$

where $R_D = c_3\big(\nu\widetilde{R}_3 + c(R_0R_1\widetilde{R}_2\widetilde{R}_3)^{1/2} + \delta_{\max}^{1/2}(\|f\| + \mu\rho_K + \mu R_K)\big)$. □

We are now ready to prove our main theoretical result stated as Theorem 1.5 in the introduction. Namely, under the above hypotheses we prove

**Theorem 4.9.** *For every $T > t_0$ that*

$$\sup\big\{\|w(t)\| : t\in[t_0,T]\big\} \to 0 \qquad \text{as} \qquad \delta\to 0.$$

*Proof.* Fix $T > t_0$. Let $t_n = t_0 + \delta n$ where $\delta \le \delta_{\max}$ and $\delta_{\max} \le T - t_0$. Let $N$ be the greatest integer such that $t_N \le T$ and consider the interval $[t_0, T]$. Taking the inner product of (4.12) with $Aw$ as in the proof of Theorem 4.4 we obtain

$$\frac{1}{2}\frac{d\|w\|^2}{dt} + \frac{1}{2}\nu|Aw|^2 \le \frac{c^2R_1R_L}{2\nu}\|w\|^2 + \mu(J(U-v),Aw). \tag{4.23}$$

Note the factor-of-two improvement in the coefficient of $\|w\|^2$ on the right comes from a different application of Young's inequality. In particular, rather than (4.16) we estimate

$$|(B(v,w),Aw) + (B(w,v),Aw)| \le \frac{c^2R_1R_L}{2\nu}\|w\|^2 + \frac{\nu}{2}|Aw|^2.$$

Upon applying the Poincaré inequality (2.3) written as $\lambda_1\|w\|^2 \le |Aw|^2$ we obtain

$$\frac{d\|w\|^2}{dt} \le C_{10}\|w\|^2 + 2\mu(w, AJ(U-v)). \tag{4.24}$$

where $C_{10} = c^2 R_1 R_L/\nu - \nu\lambda_1$.

Recall that $w(t_n) = w_n$. The definition of $w_n$ given in (4.13) implies

$$w_n = (1-\delta\mu)w(t_n^-) + \delta\mu(I-J)w(t_n^-) - \delta\mu J(U(t_n) - v(t_n)).$$

Therefore,

$$\begin{aligned}\|w_n\|^2 &= (1-\delta\mu)^2\|w(t_n^-)\|^2 + \delta^2\mu^2\|(I-J)w(t_n^-) - J(U(t_n)-v(t_n))\|^2\\ &\quad + 2\delta\mu\big(A^{1/2}(1-\delta\mu)w(t_n^-), A^{1/2}(I-J)w(t_n^-)\big)\\ &\quad - 2\delta\mu(1-\delta\mu)\big(A^{1/2}w(t_n^-), A^{1/2}J(U(t_n)-v(t_n))\big)\\ &\le (1+\delta\mu C_{11})\|w(t_n^-)\|^2 - 2\delta\mu\big(w(t_n^-), AJ(U(t_n)-v(t_n))\big) + \delta^2\mu^2 C_{12}\end{aligned}$$

where

$$C_{11} = 2 + \delta_{\max}\mu + 2c_3(1+\delta_{\max}\mu)$$

and

$$C_{12} = (M_1 + M_K + \rho_K + R_K)^2 + 2M_1(\rho_K + R_K).$$

Note for the above estimates we have used

$$(1-\delta\mu)^2 \le 1 + \delta\mu(2+\delta_{\max}\mu),$$

$$\delta^2\mu^2\|(I-J)w(t_n^-) - J(U(t_n)-v(t_n))\|^2 \le \delta^2\mu^2(M_1+M_K+\rho_K+R_K)^2,$$

$$\begin{aligned}2\big(A^{1/2}(1-\delta\mu)w(t_n^-), A^{1/2}(I-J)w(t_n^-)\big) &\le 2(1+\delta_{\max}\mu)\|w(t_n^-)\|\|(I-J)w(t_n^-)\|\\ &\le 2(1+\delta_{\max}\mu)(1+\lambda c_1 h^2)^{1/2}\|w(t_n^-)\|^2 \le 2c_3(1+\delta_{\max}\mu)\|w(t_n^-)\|^2\end{aligned}$$

and

$$2\delta^2\mu^2\big(A^{1/2}w(t_n^-), A^{1/2}J(U(t_n)-v(t_n))\big) \le 2\delta^2\mu^2 M_1(\rho_K + R_K).$$

Multiply (4.24) by the integrating factor $e^{-C_{10}t}$ to obtain

$$\frac{d}{dt}\big(e^{-C_{10}t/}\|w\|^2\big) \le 2e^{-C_{10}t}\mu(w, AJ(U-v)). \tag{4.25}$$

Now, integrate over $[t_n, t_{n+1})$ to obtain

$$\begin{aligned}
\|w(t_{n+1}^-)\|^2 &\le e^{C_{10}\delta}\|w_n\|^2 + 2\mu\int_{t_n}^{t_{n+1}} e^{C_{10}(t_{n+1}-t)}\big(w(t), AJ(U(t)-v(t))\big)dt \\
&\le e^{C_{10}\delta}\big\{(1+\delta\mu C_{11})\|w(t_n^-)\|^2 - 2\delta\mu\big(w(t_n^-), AJ(U(t_n)-v(t_n))\big) + \delta^2\mu^2 C_{12}\big\} \\
&\quad + 2\mu\int_{t_n}^{t_{n+1}} e^{C_{10}(t_{n+1}-t)}(w(t), AJ(U(t)-v(t)))dt \\
&\le e^{C_{10}\delta}\big\{(1+C_{11}\delta\mu)\|w(t_n^-)\|^2 + \delta^2\mu^2 C_{12}\big\} \\
&\quad + 2\mu\int_{t_n}^{t_{n+1}} \Big\{e^{C_{10}(t_{n+1}-t)}\big(AJ(U(t)-v(t)), w(t)\big) \\
&\qquad\qquad - e^{C_{10}\delta}\big(AJ(U(t_n)-v(t_n)), w(t_n^-)\big)\Big\}dt \\
&\le e^{C_{10}\delta}\big\{(1+C_{11}\delta\mu)\|w(t_n^-)\|^2 + \delta^2\mu^2 C_{12} + 2\mu(I_1+I_2+I_3+I_4)\big\}
\end{aligned}$$

where

$$I_1 = \int_{t_n}^{t_{n+1}} \big(e^{C_{10}(t_n-t)} - 1\big)\big(A^{1/2}J(U(t)-v(t)), A^{1/2}w(t)\big)dt,$$

$$I_2 = \int_{t_n}^{t_{n+1}} (AJ(U(t)-v(t)), w(t)-w(t_n^-))dt,$$

$$I_3 = \int_{t_n}^{t_{n+1}} \big(A^{1/2}J(U(t)-U(t_n)), A^{1/2}w(t_n^-)\big)dt$$

and

$$I_4 = -\int_{t_n}^{t_{n+1}} \big(A^{1/2}J(v(t)-v(t_n)), A^{1/2}w(t_n^-))dt.$$

Let us estimate $I_1$ first. Using (4.1) and (4.4) followed by $(e^{C_{10}\delta}-1) \le C_{10}\delta e^{C_{10}\delta}$ yields

$$\begin{aligned}
I_1 &\le \int_{t_n}^{t_{n+1}} \big(1 - e^{C_{10}(t_n-t)}\big)\big\|J(U(t)-v(t))\big\|\|w(t)\|dt \\
&\le (\rho_K + R_K)M_1 e^{-C_{10}\delta}\int_{t_n}^{t_{n+1}} \big(e^{C_{10}\delta}-1\big)dt \le \delta^2 C_{13}
\end{aligned}$$

where $C_{13} = (\rho_K + R_K)M_1 C_{10}$.

Second estimate $I_2$. Using $J = P_\lambda J$ and (2.9) with $\alpha = 2$ followed by Corollary 4.6 yields

$$\begin{aligned}
I_2 &\le \int_{t_n}^{t_{n+1}} \big|AJ(U(t)-v(t))\big||w(t)-w(t_n^-)|dt \\
&\le \int_{t_n}^{t_{n+1}} \big|AP_\lambda J(U(t)-v(t))\big||w(t)-w(t_n^-)|dt \\
&\le \int_{t_n}^{t_{n+1}} \lambda^{1/2}\big\|J(U(t)-v(t))\big\||w(t)-w(t_n^-)|dt \\
&\le \lambda^{1/2}(\rho_K + R_K)\int_{t_n}^{t_{n+1}} |w(t)-w(t_n^-)|dt \le \delta^{3/2}C_{14}
\end{aligned}$$

where $C_{14} = \lambda^{1/2}(\rho_K + R_K)M_E$.

Finally estimate $I_3$ and $I_4$ using Lemma 4.8 as

$$\begin{aligned} I_3 &\leq \int_{t_n}^{t_{n+1}} \big\|J(U(t) - U(t_n))\big\| \|w(t_n^-)\| dt \\ &\leq M_1 \int_{t_n}^{t_{n+1}} \big\|J(U(t) - U(t_n))\big\| dt \leq \delta^{3/2} C_{15} \end{aligned}$$

where $C_{15} = M_1 \rho_D$ and similarly

$$\begin{aligned} I_4 &\leq \int_{t_n}^{t_{n+1}} \big\|J(v(t) - v(t_n))\big\| \|w(t_n^-)\| dt \\ &\leq M_1 \int_{t_n}^{t_{n+1}} \big\|J(v(t) - v(t_n))\big\| dt \leq \delta^{3/2} C_{16} \end{aligned}$$

where $C_{16} = M_1 R_D$.

It follows that

$$\|w(t_{n+1}^-)\|^2 \leq e^{\delta C_{10}} \big\{ (1 + \delta\mu C_{11}) \|w(t_n^-)\|^2 + \delta^{3/2} C_{17} \big\}$$

where $C_{17} = \delta_{\max}^{1/2}(\mu^2 C_{12} + 2\mu C_{13}) + 2\mu(C_{14} + C_{15} + C_{16})$.

Setting $y_n = \|w(t_n^-)\|^2$ gives the inequality $y_{n+1} \leq \alpha y_n + \beta$ where $\alpha = e^{\delta C_{10}}(1 + \delta\mu C_{11})$ and $\beta = \delta^{3/2} e^{\delta C_{10}} C_{17}$. Note that

$$\alpha - 1 \geq \delta(C_{10} + \mu e^{\delta C_{10}} C_{11}) \qquad \text{and} \qquad \alpha^n \leq e^{(t_n - t_0)(C_{10} + \mu C_{11})}.$$

Therefore, by induction

$$\begin{aligned} \|w(t_n^-)\| &\leq e^{(t_n - t_0)(C_{10} + \mu C_{11})} \|w(t_0^-)\| + \frac{e^{(t_n - t_0)(C_{10} + \mu C_{11})} - 1}{C_{10} + \mu e^{\delta C_{10}} C_{11}} \delta^{1/2} e^{\delta C_{10}} C_{17} \\ &\leq e^{2\delta_{\max}(C_{10} + \mu C_{11})} \|w(t_0^-)\| + \frac{e^{2\delta_{\max}(C_{10} + \mu C_{11})} - 1}{C_{10} + \mu C_{11}} \delta^{1/2} e^{\delta_{\max} C_{10}} C_{17}. \end{aligned}$$

Since $\|w(t_0^-)\| = 0$ it follows there is $C_{18}$ independent of $\delta$ such that

$$\|w(t_n^-)\| \leq \delta^{1/2} C_{18} \qquad \text{for} \qquad n = 1, \ldots, N.$$

Again from (4.20) we have

$$\|w_n\| \leq (1 + \delta\mu C_4)\delta^{1/2} C_{18} + \delta\mu C_5 \leq \delta^{1/2} C_{19}$$

where $C_{19} = (1 + \delta_{\max}\mu C_4)C_{18} + \delta_{\max}^{1/2}\mu C_5$. Finally, (4.19) implies

$$\|w(t)\|^2 \leq e^{C_2\delta} \delta C_{19}^2 + \frac{C_3}{C_2}\big(e^{C_2\delta} - 1\big) \leq e^{C_2\delta}\delta C_{19}^2 + C_3 \delta e^{C_2\delta} \leq \delta C_{20}$$

where $C_{20} = e^{C_2\delta_{\max}}(C_{19}^2 + C_3)$. Therefore $\|w(t)\| \to 0$ as $\delta \to 0$ uniformly on $[t_0, T]$. $\square$

# 5 Concluding Remarks

In the context of the incompressible two-dimensional Navier–Stokes equations we have introduced a relaxation parameter $\kappa$ depending on the time $\delta$ between successive observations into the update step of the spectrally-filtered direct-insertion method. This overcomes the lack of synchronization when the observations are inserted too frequently. The relationship between $\kappa$ and $\delta$ may be obtained numerically by varying these parameters independently and then minimizing the average error about an ensemble of reference solutions. It turns out that the relation $\kappa = \mu\delta$ for a particular fixed $\mu$ works well over a wide range.

Analytically we have shown as $\delta \to 0$ that the approximation corresponding to the $\kappa$-relaxed discrete-in-time method with $\kappa = \mu\delta$ converges to the solution obtained by continuous nudging on any finite time interval. Although this does not imply $\|\tilde{u}(t) - U(t)\| \to 0$ as $t \to \infty$ for all sufficiently small $\delta$, the numerics suggest for suitable $h$, $\lambda$ and $\mu$ that $\tilde{u}$ does indeed synchronize with $U$. Analysis proving such a result would be of great interest.

Much of the difficulty overcome by the relaxation factor $\kappa$ results from the fact that $J$ is not a projection but rather a filtered version of the interpolant $I_h$. An alternative approach was introduced by Li, Hawkins, Rebholz and Vargun [19] in the context of finding stationary solutions to the Navier–Stokes equations. Namely, nudge with $J^*J$ rather than $J$ directly. In our case this would lead to an update step of the form

$$u_{n+1} = (I - \kappa J^*J)S(t_{n+1} - t_n)u_n + \kappa J^*JU(t_{n+1}).$$

We intend to explore the simulation and analysis of this method in future work.

Data assimilation for the two-dimensional magnetohydrodynamic equations studied by Biswas, Hudson, Larios and Pei [3] and Hudson and Jolly [21] provide an opportunity to further test the scaling $\kappa = \delta\mu$. Let $\mathbf{S}$ be the semigroup corresponding to the evolution of the two-dimensional magnetohydrodynamic equations and $\mathbf{X} = (U_1, U_2, B_1, B_2)$ be the state of the velocity and magnetic fields. Given the free-running solution $\mathbf{X}(t) = \mathbf{S}(t)\mathbf{X}_0$ consider interpolated observations $\mathbf{JX}(t_n)$ at times $t_n$ taken on one component of each field. Thus,

$$\mathbf{J}(u_1, u_2, b_1, b_2) = (Ju_1, 0, Jb_1, 0)$$

where $Ju_1$ and $Jb_1$ could be projections onto the $N$ lowest Fourier modes or interpolants of the form $P_\lambda P_H I_h$ as in (2.10). The analysis step corresponding to (1.2) then becomes

$$\tilde{\mathbf{x}}_{n+1} = (I - \delta\mu\mathbf{J})\mathbf{S}(t_{n+1} - t_n)\tilde{\mathbf{x}}_n + \delta\mu\mathbf{JX}(t_n).$$

Our conjecture is that $\tilde{\mathbf{x}}_n$ will as $\delta \to 0$ converge to the approximating solutions obtained by the continuous-in-time nudging method given as Algorithm 2.3 in [21].

In the more general case the time between successive observations may not be uniform. For example, the time $\delta_n = t_{n+1} - t_n$ between successive observations might be small for most of the time but occasionally large due to missing observations. Taking $\kappa_n = \min(1, \delta_n\mu)$ would avoid over-relaxation and provided there are not many gaps where $\delta_n$ is large it is plausible the approximating solution would still synchronize with the reference solution.

# References


[1] Argonne National Laboratory and the University of Illinois: "MPICH: High-Performance Portable MPI". `www.mpich.org`. Accessed: 10 May 2023.

[2] Azouani, A., Olson, E., Titi, E.S.: Continuous data assimilation using general interpolant observables. *Journal of Nonlinear Science* **24**(2), 277–304 (2014).

[3] Biswas, A., Hudson, J., Larios, A., Pei, Y.: Continuous data assimilation for the magnetohydrodynamic equations in 2D using one component of the velocity and magnetic fields. *Asymptotic Analysis* **108**, 1–43 (2018).

[4] Carlson, E., Farhat, A., Martinez, V.R., Victor, C.: Assimilation in the limit of infinite error feedback gain. arXiv:2408.02646v2 (2025).

[5] Celik, E., Olson, E.: Data assimilation using time-delay nudging in the presence of Gaussian noise. *Journal of Nonlinear Science* **33**(110), 1–31 (2023).

[6] Celik, E., Olson, E., Titi, E.S.: Spectral filtering of interpolant observables for a discrete-in-time downscaling data assimilation algorithm. *SIAM Journal on Applied Dynamical Systems* **18**(2), 1118–1142 (2019).

[7] Constantin, P., Foias, C.: *Navier–Stokes Equations*. Chicago Lectures in Mathematics, University of Chicago Press, Chicago, IL (1988).

[8] Cox, S.M., Matthews, P.C.: Exponential time differencing for stiff systems. *Journal of Computational Physics* **176**, 430–455 (2002).

[9] Diegel, A.E., Li, X., Rebholz, L.G.: Analysis of continuous data assimilation with large (or even infinite) nudging parameters. *Journal of Computational and Applied Mathematics* **456**, 16 pages (2025).

[10] Evensen, G.: *Data Assimilation: The Ensemble Kalman Filter*. Springer, Berlin (2007).

[11] Farhat, A., Lunasin, E., Titi, E.S.: Abridged continuous data assimilation for the 2D Navier–Stokes equations utilizing measurements of only one component of the velocity field. *Journal of Mathematical Fluid Mechanics* **18**(1), 1–23 (2016).

[12] Farhat, A., Glatt-Holtz, N.E., Martinez, V.R., McQuarrie, S.A., Whitehead, J.P.: Data assimilation in large Prandtl Rayleigh–Bénard convection from thermal measurements. *SIAM Journal on Applied Dynamical Systems* **19**(1), 510–540 (2020).

[13] Foias, C., Manley, O., Rosa, R., Temam, R.: *Navier–Stokes Equations and Turbulence*, Volume 83. Cambridge University Press (2001).

[14] Foias, C., Mondaini, C.F., Titi, E.S.: A discrete data assimilation scheme for the solutions of the two-dimensional Navier–Stokes equations and their statistics. *SIAM Journal on Applied Dynamical Systems* **15**(4), 2109–2142 (2016).

[15] Frigo, M., Johnson, S.G.: The design and implementation of FFTW3. *Proceedings of the IEEE* **93**(2), 216–231 (2005).

[16] The Free Software Foundation: "GCC, the GNU Compiler Collection". `gcc.gnu.org`. Accessed: 10 May 2023.

[17] Grudzien, C., Bocquet, M.: A tutorial on Bayesian data assimilation. *Applications of Data Assimilation and Inverse Problems in the Earth Sciences*, Chapter 3, pp. 27–48. Cambridge University Press (2023).

[18] Hammoud, M.A.E.R., Le Maître, O., Titi, E.S., Hoteit, I., Knio, O.: Continuous and discrete data assimilation with noisy observations for the Rayleigh-Bénard convection: A computational study. *Computational Geosciences* **27**, 63–79 (2023).

[19] Li, X., Hawkins, E.V., Rebholz, L.G., Vargun, D.: Accelerating and enabling convergence of nonlinear solvers for Navier–Stokes equations by continuous data assimilation. *Computer Methods in Applied Mechanics and Engineering* **416**, 116313 (2023).

[20] Hayden, K., Olson, E., Titi, E.S.: Discrete data assimilation in the Lorenz and 2D Navier–Stokes equations. *Physica D* **240**(18), 1416–1425 (2011).

[21] Hudson, J., Jolly, M.S.: Numerical efficacy study of data assimilation for the 2D magnetohydrodynamic equations. *Journal of Computational Dynamics* **6**(1), 131–145 (2019).

[22] Jolly, M.S., Martinez, V.R., Titi, E.S.: A data assimilation algorithm for the 2D subcritical surface quasi-geostrophic equation. *Advances in Nonlinear Studies* **17**, 167–192 (2017).

[23] Jolly, M.S., Martinez, V.R., Olson, E.J., Titi, E.S.: Continuous data assimilation with blurred-in-time measurements of the surface quasi-geostrophic equation. *Chinese Annals of Mathematics, Series B* **40**, 721–764 (2019).

[24] Jones, D.A., Titi, E.S.: Determining finite volume elements for the 2D Navier–Stokes equations. *Physica D* **60**, 165–174 (1992).

[25] Kassam, A., Trefethen, L.N.: Fourth-order time-stepping for stiff PDEs. *SIAM Journal on Scientific Computing* **26**(4), 1214–1233 (2005).

[26] Larios, A., Pei, Y., Victor, C.: The second-best way to do sparse-in-time continuous data assimilation: Improving convergence rates for the 2D and 3D Navier–Stokes equations. arXiv:2303.03495v1 (2023).

[27] Olson, E., Titi, E.S.: Determining modes for continuous data assimilation in 2D turbulence. *Journal of Statistical Physics* **113**(5–6), 799–840 (2003).

[28] Robinson, J.C.: *Infinite-Dimensional Dynamical Systems*. Cambridge Texts in Applied Mathematics, Cambridge University Press, Cambridge (2001).

[29] Temam, R.: *Navier–Stokes Equations. Theory and Numerical Analysis*. Studies in Mathematics and its Applications, Vol. 2. North-Holland Publishing Co., Amsterdam–New York–Oxford (1977).

[30] Titi, E.S.: On a criterion for locating stable stationary solutions to the Navier–Stokes equations. *Nonlinear Analysis: Theory, Methods & Applications* **11**(9), 1085–1102 (1987).